

Elliptical plasma-filled waveguide as a new standard short-period undulator

Mansour Hadad,^{a,b} Sirous Yousefnejad,^b Farhad Saeidi,^b Javad Rahighi^b and Babak Shokri^{a*}

^aDepartment of Physics, Shahid Beheshti University, Tehran, Iran, and ^bIranian Light Source Facility, Institute for Research in Fundamental Sciences (IPM), Tehran, Iran. *Correspondence e-mail: b-shokri@sbu.ac.ir

Received 14 November 2020

Accepted 22 April 2021

Edited by S. Svensson, Uppsala University, Sweden

Keywords: undulator; plasma-filled waveguide; elliptical waveguide; synchrotron radiation.

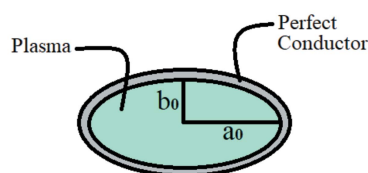
Undulators as the sources of high-brilliance synchrotron radiation are of widespread interest in new generations of light sources and free-electron lasers. Microwave propagation in a plasma-filled elliptical waveguide can be studied as a standard short-period undulator. This structure as a lucrative insertion device can be installed in the storage ring of third- and fourth-generation light sources to produce high-energy and high-brilliance synchrotron radiation. In this article, the propagation of the transverse electric modes in a plasma-filled waveguide with an elliptical cross-section is investigated, and the field components, the cut-off frequencies and the electron beam trajectory are calculated. With due consideration of the electron beam dynamics and in order to achieve a standard short-period undulator, parameters such as the dimensions of the waveguide elliptical cross-section, the microwave frequency and the plasma density are calculated.

1. Introduction

Synchrotron radiation has many applications in different branches of science such as physics, chemistry, biology, materials science, medicine, *etc.* (Onuki & Elleaume, 2003). Undulators and wigglers are the foremost sources of synchrotron radiation in light source facilities and free-electron lasers (FELs). Undulators can generate synchrotron radiation with higher photon flux and higher brightness than wigglers (Clarke, 2004). In recent years, many attempts have been made to design new generations of undulators capable of generating photons with higher energy and higher brightness. The energy of generated synchrotron radiation photons in an undulator is a function of the undulator period length and deflection parameter as

$$\varepsilon_{\text{ph}} [\text{eV}] = 950 \frac{n E^2 [\text{GeV}]}{\lambda_u [\text{cm}] [1 + (K^2/2) + \gamma^2 \theta^2]},$$

where n is the harmonic number, E is the electron beam energy, λ_u is the period length, K is the deflection parameter, γ is the Lorentz factor, and θ is the observation angle. The synchrotron radiation flux generated on an undulator axis ($\theta = 0$) depends on the undulator deflection parameter in the form of $\varphi_n = 1.43 \times 10^{14} N_p I Q_n(K)$, where N_p is the undulator number of periods, I is the electron beam current in ampere, and $Q_n(K)$ is a function of the deflection parameter. When the deflection parameter decreases ($K < 1$), $Q_n(K)$ decreases to zero especially for higher harmonics, and when the deflection parameter increases, $Q_n(K)$ increases and reaches its maximum for $K \simeq 5$ and remains almost constant for larger deflection parameters (Clarke, 2004).



The deflection parameter depends on the undulator period length and magnetic field as $K = 0.934 B_u [\text{T}] \lambda_u [\text{cm}]$, which signifies the fact that period length reduction leads to a reduction of the deflection parameter. There are two ways to generate synchrotron radiation with higher energy: increasing the electron beam energy or reducing the undulator period length. Period length reduction, besides its lower cost, provides the ability to generate higher photon flux in incorporating more periods in insertion devices (IDs) or installing more IDs within the available space in the straight sections of light source facilities and FELs. So, many attempts have been made to design new undulators with shorter period lengths, such as in-vacuum undulators (IVUs) ($\lambda_u \simeq 10 \text{ mm}$) (Chavanne *et al.*, 2003; Huang *et al.*, 2014; Kitamura, 1995), cryogenic permanent magnets undulators (CPMUs) ($\lambda_u \simeq 10 \text{ mm}$) (Benabderrahmane *et al.*, 2017; Chavanne *et al.*, 2008; Hara *et al.*, 2004; Tanaka *et al.*, 2006), microwave undulators (MUs) ($\lambda_u \simeq 1 \text{ mm}$) (Batchelor, 1986; Kuzikov *et al.*, 2013; Pellegrini, 2005; Tantawi *et al.*, 2014), crystalline undulators ($\lambda_u \simeq 100 \text{ nm}$) (Bellucci *et al.*, 2003) and plasma undulators ($\lambda_u \simeq 1 \text{ mm}$) (Corde & Ta Phuoc, 2011; Joshi *et al.*, 1987; Rykovanov *et al.*, 2015). However, achieving shorter period length generally comes at a price. Most of these undulators have very small deflection parameters ($K < 1$) which leads to a reduction of photon flux and brilliance. It also inevitably results in the separation of the harmonics of undulators' tuning curves.

The deflection parameter of an undulator with overlapping radiated harmonics and continuous energy spectrum is larger than two ($K > 2$). Such an undulator has been called a 'standard undulator' (Huang *et al.*, 2017). Separation of the harmonics, due to the period length reduction, gives rise to non-standard undulators.

In order to tackle this problem in IDs with permanent-magnet structures such as CPMUs and IVUs, a strong magnetic field and, therefore, permanent-magnet blocks with high magnetic remanence field are required. Permanent magnets in CPMUs are cooled down to cryogenic temperatures and therefore their remanence is improved significantly, but the highest accessible remanence field is bounded up to 1.7 T. To achieve a stronger magnetic field, it is also possible to decrease the undulators' magnetic gap. However, the minimum accessible magnetic gap is bounded to the beam stay-clear. In fact, due to these limitations, the period length of a standard permanent magnet undulator (PMU) could not be smaller than 10 mm.

In an MU, the electromagnetic field of the microwave radiation is responsible for the electron's wiggling motion (Tantawi *et al.*, 2014), and to reduce its period length the microwave frequency needs to be increased. Though it is possible to attenuate to some extent the undesirable effect of period length reduction on the deflection parameter through increasing the microwave intensity, a very high microwave intensity may result in an electrical breakdown in the MU's vacuum waveguides. In fact, the deflection parameters of short-period MUs are smaller than two ($K < 2$) and these undulators are non-standard undulators.

To prevent electrical breakdown, the idea of using plasma-filled waveguides is investigated here. Using plasma makes it possible to amplify the microwave intensity in order to reach a shorter period length while avoiding the electrical breakdown. In other words, to keep $K > 2$ in short-period MUs, microwave undulators with plasma-filled waveguides, hereafter called microwave plasma undulators (MPUs), are proposed and investigated in this work.

In an MPU, high-power and high-frequency microwave radiation propagate in a plasma-filled waveguide, and the electromagnetic fields of the microwave radiation makes the electron beam oscillate and generate synchrotron radiation. In this work, an introduction to MPUs is given and the advantages of using an elliptical plasma-filled waveguide compared with conventional undulators are given. MPUs are similar to MUs except for the plasma in their waveguides. This means that the way of using an MPU is similar to that of an MU, and previous studies concerning different aspects of accelerator physics of MUs are applicable to MPUs. The only substantial difference is plasma in their waveguides and its effect on the electron beam quality through electron-plasma interactions. This effect is investigated here and parameters such as the emittance and the energy spread of an electron beam in a plasma-filled waveguide are calculated. The calculation of other parameters such as the stored energy, shunt impedance, filling time and quality factor which are essential for designing accelerator cavities are not under the scope of this work. These parameters could be investigated in detail in a future study to find their optimum values and to select the best shape and dimensions of a plasma-filled waveguide. For example, a circular corrugated or an elliptical corrugated plasma-filled waveguide could be studied for this purpose (Zhang *et al.*, 2019). However, regarding the use of a plasma-filled waveguide as a short-period undulator, it can be mentioned that, after installing the waveguide in a storage ring, an appropriate gas should be injected to produce plasma inside it. Because the plasma generation method depends on the gas density and temperature, the gas should be converted to plasma using a plasma generation method (like microwave heating) that is appropriate for the storage ring condition (Wong & Mongkolnarin, 2016; Smirnov, 2015). The waveguide is then ready for the injection of high-intensity microwaves to create a standing wave in it. The electromagnetic fields of the standing wave cause the electron beam to oscillate and produce synchrotron radiation.

Due to the electron-plasma interactions in plasma-filled waveguides, there might be a concern about the beam quality degradation and increased beam emittance and energy spread. Since the beam quality degradation is a function of the electron beam and plasma properties, attempts have been made to limit it by choosing suitable parameters for plasma to maintain the emittance and the energy spread of the electron beam in an acceptable range of the beam dynamics of fourth-generation light sources.

Even though increasing the microwave frequency can pave the way for reaching undulators with shorter period length, it may also result in the excitation of higher-order harmonics

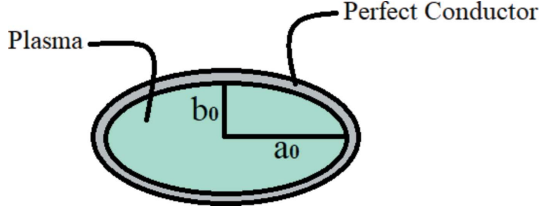


Figure 1
Elliptical cross-section of an MPU with $a_0 = 6$ mm and $b_0 = 2.1$ mm.

and therefore in the reduction of undulator efficiency. To excite only the basic mode in an undulator while increasing the microwave frequency, the waveguide cross-section should be reduced. The minimum accessible cross-section of a waveguide is confined to the horizontal and the vertical beam stay-clear (BSC) of the beam. The horizontal and the vertical BSC of the Iranian Light Source Facility (ILSF) storage ring are 6 mm and 2.1 mm, respectively. This means that the smallest allowed circular waveguide diameter is 6 mm. For such a circular waveguide, the cut-off frequencies of the basic mode (TE₁₁) and the next two modes (TM₀₁ and TE₂₁) are 14.64 GHz, 19.13 GHz and 24.29 GHz, respectively. So, to excite only the basic mode, the microwave frequency inside the waveguide should not be higher than 19.13 GHz. The period length of the TE₁₁ mode in such a circular waveguide with a cut-off frequency of 19.13 MHz is 9.9 mm. It is possible to use smaller cross-sections by using elliptical waveguides. In an elliptical waveguide, it is possible to set one of the semi-axis dimensions to 2.1 mm (vertical beam stay clear) and set the other one to 6 mm (horizontal beam stay clear) (Fig. 1). The cut-off frequencies of the basic mode and the next two modes of this elliptical waveguide are 14.64 GHz, 27.19 GHz and 38.71 GHz, respectively.

Using plasma, in addition to providing the possibility of applying higher microwave intensities, increases the cut-off frequencies of different modes. For example, the cut-off frequencies of the basic mode and the next two modes of the elliptical waveguide in Fig. 1, filled by cold plasma with a density of $n_0 = 3.1 \times 10^{14} \text{ cm}^{-3}$, are 96.61 GHz, 177.5 GHz and 253 GHz, respectively. Therefore, it is possible to increase the applied microwave frequency up to 177.5 GHz without exciting the higher modes and without reducing the quality of the electron beam. This increase in the microwave frequency makes it possible to achieve undulators with shorter period length.

In the following, an elliptical plasma-filled waveguide with the electron beam characteristics of the ILSF storage ring is investigated, and the transverse electric (TE) mode field components of the microwave radiation, the electron wiggling motion, the deflection parameter, the period length, the photon flux and the spectrum of this waveguide are calculated.

2. TE mode field components

As defined by the standard hydrodynamic model, the dielectric tensor of a cold collision-less unmagnetized plasma is (Krall & Trivelpiece, 1973)

$$\epsilon = \epsilon_0 \begin{bmatrix} \epsilon_{11} & 0 & 0 \\ 0 & \epsilon_{22} & 0 \\ 0 & 0 & \epsilon_{33} \end{bmatrix}, \quad (1)$$

$$\epsilon_{11} = 1 - \frac{\omega_p^2}{\omega^2} = \epsilon_{22} = \epsilon_{33} = \epsilon_{\text{eff}}, \quad (2)$$

$$\omega_p = \left(\frac{n_0 e^2}{\epsilon_0 m_e} \right)^{1/2}, \quad (3)$$

where ω is the microwave frequency, ω_p is the electron-plasma frequency, and n_0 is the plasma density. Considering the elliptical waveguide in Fig. 1 and assuming the direction of propagation to be along the z -axis, the relations between the elliptic coordinates and their rectangular counterparts are given as (McLachlan, 1951)

$$x = d \cosh \xi \cos \eta, \quad y = d \sinh \xi \sin \eta, \quad z = z, \quad (4)$$

where $0 \leq \xi \leq \xi_0 = \tanh^{-1}(b_0/a_0)$, $0 \leq \eta \leq 2\pi$, and $d = (a_0^2 - b_0^2)^{1/2}$ is the semi-focal length of the ellipse. The axis of the elliptical waveguide is considered to be at the origin. To calculate the TE mode field components of this waveguide, the dielectric tensor is inserted into Maxwell's equations, the boundary conditions of a complete plasma-filled elliptical waveguide surrounded by a perfect conduction material are applied, and the fact that E_z is equal to zero for the TE mode field components is considered,

$$\nabla^2 B_z + \frac{\omega^2}{c^2} \epsilon_{\text{eff}} B_z = 0. \quad (5)$$

The behavior of the electric and the magnetic field components along the waveguide axis is as $\exp(\pm i\beta z)$. Using equation (5) for the electrical field along the z -axis gives

$$\frac{1}{l^2} \left(\frac{\partial^2}{\partial \xi^2} + \frac{\partial^2}{\partial \eta^2} \right) B_z + k_c^2 B_z = 0, \quad (6)$$

where $k_c^2 = (\omega^2/c^2) \epsilon_{\text{eff}} - \beta^2$ and $l = d(\cosh^2 \xi - \cos^2 \eta)^{1/2}$. Equation (6) is a differential equation, known as the Mathieu differential equation, with a well known solution and eigenvalue (McLachlan, 1951) as

$$B_z = \sum_{m=0}^{\infty} C_m C e_m(\xi, q) c e_m(\eta, q) + \sum_{m=1}^{\infty} S_m S e_m(\xi, q) s e_m(\eta, q), \quad (7)$$

where $c e_m(\eta, q)$ and $s e_m(\eta, q)$ are the even and the odd solutions of the angular Mathieu equation, $C e_m(\xi, q)$ and $S e_m(\xi, q)$ are the even and the odd solutions of the radial Mathieu equation of the first kind, and C_m and S_m are computable arbitrary constants. For any m , there are even and odd solutions in the following form,

$$B_{zme} = C_m C e_m(\xi, q) c e_m(\eta, q), \quad (8)$$

$$l = d(\cosh^2 \xi - \cos^2 \eta)^{1/2}. \quad (9)$$

Given the boundary condition $E_\eta(\xi_0, \eta) = \partial B_z / \partial \xi|_{\xi_0} = 0$, then $C e'_m(\xi_0, q) = 0$ and $S e'_m(\xi_0, q) = 0$. Considering $q_{m,r}$ and $\bar{q}_{m,r}$ as

the r th root of $Ce'_m(\xi_0, q)$ and $Se'_m(\xi_0, q)$, respectively, therefore

$$B_{zme} = C_{m,r} Ce_m(\xi, q_{m,r}) ce_m(\eta, q_{m,r}) \exp[-i(\omega t \pm \beta z)], \quad m \geq 0, r \geq 1, \quad (10)$$

$$B_{zms} = S_{m,r} Se_m(\xi, \bar{q}_{m,r}) se_m(\eta, \bar{q}_{m,r}) \exp[-i(\omega t \pm \beta z)], \quad m \geq 1, r \geq 1, \quad (11)$$

and the TE_{mr} field components are

$$E_{\xi me} = \frac{-i\omega}{k_c^2(e)l} C_{m,r} Ce_m(\xi, q_{m,r}) ce'_m(\eta, q_{m,r}) \exp[-i(\omega t \pm \beta z)], \quad (12)$$

$$E_{\xi ms} = \frac{-i\omega}{k_c^2(s)l} S_{m,r} Se_m(\xi, \bar{q}_{m,r}) se'_m(\eta, \bar{q}_{m,r}) \exp[-i(\omega t \pm \beta z)], \quad (13)$$

$$E_{\eta me} = \frac{i\omega}{k_c^2(e)l} C_{m,r} Ce'_m(\xi, q_{m,r}) ce_m(\eta, q_{m,r}) \exp[-i(\omega t \pm \beta z)], \quad (14)$$

$$E_{\eta ms} = \frac{i\omega}{k_c^2(s)l} S_{m,r} Se'_m(\xi, \bar{q}_{m,r}) se_m(\eta, \bar{q}_{m,r}) \exp[-i(\omega t \pm \beta z)], \quad (15)$$

$$B_{\xi me} = \frac{-i\beta}{k_c^2(e)l} C_{m,r} Ce'_m(\xi, q_{m,r}) ce_m(\eta, q_{m,r}) \exp[-i(\omega t \pm \beta z)], \quad (16)$$

$$B_{\xi ms} = \frac{-i\beta}{k_c^2(s)l} S_{m,r} Se'_m(\xi, \bar{q}_{m,r}) se_m(\eta, \bar{q}_{m,r}) \exp[-i(\omega t \pm \beta z)], \quad (17)$$

$$B_{\eta me} = \frac{-i\beta}{k_c^2(e)l} C_{m,r} Ce_m(\xi, q_{m,r}) ce'_m(\eta, q_{m,r}) \exp[-i(\omega t \pm \beta z)], \quad (18)$$

$$B_{\eta ms} = \frac{-i\beta}{k_c^2(s)l} S_{m,r} Se_m(\xi, \bar{q}_{m,r}) se'_m(\eta, \bar{q}_{m,r}) \exp[-i(\omega t \pm \beta z)], \quad (19)$$

where β is the propagation constant given by $\beta = [(\omega/c)^2 \epsilon_{\text{eff}} - k_c^2(e, s)]^{1/2}$ with $k_c^2(e) = 4(q_{m,r}/d^2)$ and $k_c^2(s) = 4(\bar{q}_{m,r}/d^2)$. The corresponding cut-off frequency and wave-number are

$$f_c(e) = \frac{c(q_{m,r})^{1/2}}{d\pi(\epsilon_{\text{eff}})^{1/2}}, \quad f_c(s) = \frac{c(\bar{q}_{m,r})^{1/2}}{d\pi(\epsilon_{\text{eff}})^{1/2}}, \quad k_c = \frac{\omega_c(\epsilon_{\text{eff}})^{1/2}}{c}, \quad (20)$$

where (e) and (s) refer to even and odd modes. It can be seen that the cut-off frequency (f_c) depends on the waveguide dimensions. The electromagnetic field components perpendicular to the direction of propagation are

$$E_{\perp} = -\frac{i\omega}{k_c^2} B_{0e,s} G_{e,s}(\xi, \eta) \exp[-i(\omega t \pm \beta z)], \quad (21)$$

$$B_{\perp} = -\frac{i\beta}{k_c^2} B_{0e,s} G_{e,s}(\xi, \eta) \exp[-i(\omega t \pm \beta z)], \quad (22)$$

where

$$G_e(\xi, \eta) = \frac{1}{l} \left\{ [Ce_m(\xi, q_{m,r}) ce'_m(\eta, q_{m,r})]^2 + [Ce'_m(\xi, q_{m,r}) ce_m(\eta, q_{m,r})]^2 \right\}^{1/2}, \quad (23)$$

$$G_s(\xi, \eta) = \frac{1}{l} \left\{ [Se_m(\xi, q_{m,r}) se'_m(\eta, q_{m,r})]^2 + [Se'_m(\xi, q_{m,r}) se_m(\eta, q_{m,r})]^2 \right\}^{1/2}. \quad (24)$$

In Fig. 2, the electric field patterns of the first three modes of the plasma-filled elliptical waveguide are plotted by CST Studio (CST Microwave Studio, 2008) software. In an elliptical waveguide, the cut-off frequency of the even TE_{11} mode is smaller than those of the other modes and therefore this mode is the dominant mode.

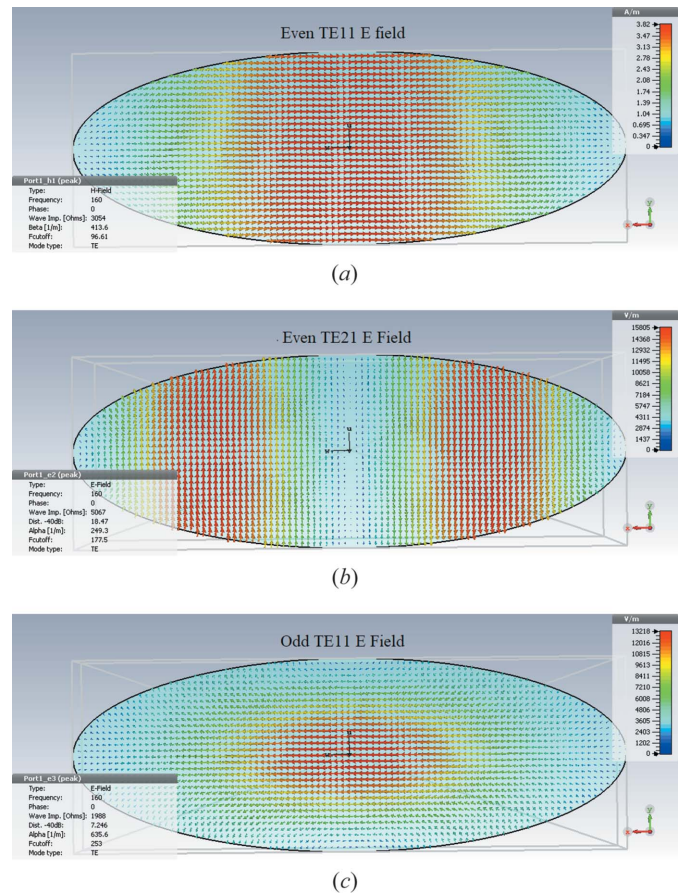


Figure 2 The electric field pattern of the first three modes of the elliptical waveguide ($a_0 = 6$ mm and $b_0 = 2.1$ mm) filled with the cold plasma with $n_0 = 3.1 \times 10^{14}$ cm $^{-3}$, $\omega_p = 9.932 \times 10^{11}$ rad s $^{-1}$, $f = 160$ GHz, and $\epsilon_{\text{eff}} = 0.024$.

3. Period length and deflection parameter

The period length, the deflection parameter and the number of periods are the main parameters used to obtain the synchrotron radiation characteristics of an ID, such as energy, flux and brilliance. Electromagnetic fields are responsible for the electron undulating trajectory inside waveguides. The period length of the electron undulating trajectory and the maximum transverse deflection angle are regarded as the undulator period length and deflection parameter, respectively.

Considering a moving electron along the z -axis with the speed of V_z , the Lorentz force and its component along the x -direction are

$$F = -e(E + V \times B), \quad (25)$$

$$F_x = \gamma m_0 \frac{d^2x}{dt^2} = -e(E_x - V_z B_y), \quad (26)$$

where $E_x = E_{1x} \sin(\beta z) \sin[(\omega/c)z]$ and $B_y = B_{1y} \cos(\beta z) \cos[(\omega/c)z]$, $E_{1x} = E_{\perp} \cos(\eta)$ and $B_{1y} = B_{\perp} \cos(\eta)$ are the electric and the magnetic field peaks and $B_{\perp} = (\beta/\omega)E_{\perp}$. Substituting E_x and B_y into equation (26) gives

$$F_x = \frac{eE_{1x}}{2} \left\{ \left(\frac{\lambda_0}{\lambda_g} + 1 \right) \cos \left[2\pi z \left(\frac{\lambda_g + \lambda_0}{\lambda_0 \lambda_g} \right) \right] + \left(\frac{\lambda_0}{\lambda_g} - 1 \right) \cos \left[2\pi z \left(\frac{\lambda_g - \lambda_0}{\lambda_0 \lambda_g} \right) \right] \right\}, \quad (27)$$

where $\lambda_0 = 2\pi c/\omega$ and $\lambda_g = 2\pi/\beta$ are the wavelength of microwave in free space and in the waveguide, respectively. The first term in equation (27) is responsible for the counter-propagating mode and the second term is responsible for the co-propagating mode. The period length in the counter-propagating and in the co-propagating modes for relativistic electrons are

$$\lambda_{u\text{-counter}} = \frac{\lambda_0 \lambda_g}{\lambda_g + \lambda_0} = \frac{2\pi c}{\omega} \times \frac{1}{1 + (\epsilon_{\text{eff}})^{1/2} \left(1 - \frac{c^2 k_z^2}{\omega^2 \epsilon_{\text{eff}}} \right)^{1/2}}, \quad (28)$$

$$\lambda_{u\text{-co}} = \frac{\lambda_g \lambda_0}{\lambda_g - \lambda_0} = \frac{2\pi c}{\omega} \times \frac{1}{1 - (\epsilon_{\text{eff}})^{1/2} \left(1 - \frac{c^2 k_z^2}{\omega^2 \epsilon_{\text{eff}}} \right)^{1/2}}. \quad (29)$$

The counter-propagating mode generates the desired high-frequency wiggling motion of electrons which in turn results in the generation of synchrotron radiation with higher energy compared with the co-propagating mode. Therefore, the counter-propagating mode is more favorable. For $\lambda_0 \cong \lambda_g$ the effect of the co-propagating mode on the electron beam vanishes which means $(\omega/c) \epsilon_{\text{eff}} \gg k_c$. Using the first term in equation (27) to calculate the deflection parameter gives

$$\frac{dx}{dz} = \frac{eE_1}{2\pi\gamma m_0 c^2} \left(\frac{\lambda_g}{\lambda_g + \lambda_0} \right) \left(\frac{\lambda_g + \lambda_0}{\lambda_0 \lambda_g} \right) \sin(\Delta z), \quad (30)$$

$$K_x = \left| \left(\gamma \frac{dx}{dz} \right)_{\text{max}} \right| = \frac{eE_{1x}}{4\pi m_0 c^2} \left(\frac{\lambda_0 \lambda_g}{\lambda_g + \lambda_0} \right) \left(\frac{\lambda_g + \lambda_0}{\lambda_g} \right), \quad (31)$$

so we have

$$K_x = 0.934 \frac{E_{1x}}{2c} \lambda_0 \equiv 0.934 B_u [T] \lambda_u [\text{cm}], \quad (32)$$

where

$$B_u = \frac{E_{1x}}{2c} \left(\frac{\lambda_g + \lambda_0}{\lambda_g} \right), \quad (33)$$

$$\lambda_u = \left(\frac{\lambda_0 \lambda_g}{\lambda_g + \lambda_0} \right). \quad (34)$$

Similarly, for the Lorentz force along the y -direction, the deflection parameter of the vertical oscillation along the y -axis is

$$K_y = \left| \left(\gamma \frac{dy}{dz} \right)_{\text{max}} \right| = \frac{eE_{1y}}{4\pi m_0 c^2} \left(\frac{\lambda_0 \lambda_g}{\lambda_g + \lambda_0} \right) \left(\frac{\lambda_g + \lambda_0}{\lambda_g} \right) = 0.934 \frac{E_{1y}}{2c} \lambda_0, \quad (35)$$

where $E_{1y} = E_{\perp} \sin(\eta)$.

4. Numerical results and calculations

The plasma density and the microwave frequency are significant in MPUs. MPUs are proposed to reach standard undulators with shorter period length compared with conventional MUs. As mentioned before, to obtain a shorter period length, the microwave frequency needs to be increased, and, in addition to technical limitations, other considerations need to be taken into account. For example, to prevent detrimental effects of higher propagating modes on the electron beam dynamics, the frequency should be chosen so that only the dominant mode will be excited.

Using plasma instead of vacuum makes it possible to increase the cut-off frequencies of propagating modes. There is a direct relationship between the plasma frequency and the cut-off frequencies, *i.e.* the higher the plasma frequency, the higher the cut-off frequencies will be. However, high plasma density is a prerequisite of high plasma frequency, but high plasma density adversely affects the electron beam dynamics. So there should be a trade-off between increasing plasma density and degradation of beam quality.

Beam quality degradation results from two main sources: beam instabilities due to the beam-plasma interactions and wake fields. Two significant instabilities are raised, called Two-Stream and Weible instabilities. The growth rate of the Two-Stream instability is proportional to the electron beam density and the plasma density in the form of $\delta \simeq (n_b/n_0)^{1/3} (\omega_p/\gamma)$, where n_b is the density of the electron beam, n_0 is the density of the plasma, and γ is the Lorentz factor. If the e-folding length of this instability is larger than the beam length [$L \leq \gamma (n_0/n_b)^{1/3} (c/\omega_p)$], the Two-Stream instability will be constant (Joshi *et al.*, 1987). A single bunch of electrons inside the ILSF storage ring with $n_b \simeq 8.6 \times 10^{17} \text{ cm}^{-3}$ and $\gamma = 5870$ has a length of about 8 mm. Therefore, to prevent the Two-Stream instability, the plasma density (n_0) should be less than $4.76 \times 10^{21} \text{ cm}^{-3}$ and the plasma frequency (ω_p) should be smaller than $3.89 \times 10^{15} \text{ rad s}^{-1}$.

The Weible instability is a purely transverse instability responsible for the filamentation of wide beams in plasma. Although this instability is not suppressed for short bunches, it is suppressed mainly for bunches narrower than the plasma skin depth, *i.e.* narrower than c/ω_p . To avoid the Weible instability for the ILSF storage ring electron beam (an ultra-low emittance beam with small horizontal and vertical beam sizes of $\sigma_x = 68.9 \mu\text{m}$ and $\sigma_y = 2.96 \mu\text{m}$), plasma density (n_0) should be less than $6.2 \times 10^{16} \text{cm}^{-3}$ and the plasma frequency (ω_p) should be smaller than $4.4 \times 10^{12} \text{rad s}^{-1}$.

In addition to the beam–plasma instabilities, the wake field can also degrade the electron beam quality. The longitudinal and the radial wake forces affect the energy spread and the emittance of the electron beam, respectively. The radial wake force exerts a pinching force on the beam. This force might be used to focus the electron beam in some cases, such as a plasma lens, but in MPUs it leads to undesirable angular variation and emittance growth. In vacuum, the radial repulsion of a relativistic electron beam space charge is canceled by the beam’s own azimuthal magnetic field, and therefore the radial repulsion does not increase the beam emittance. In plasma, the plasma electrons are expelled by the beam space charge and therefore the beam space charge radial repulsion is neutralized by the plasma ions. However, due to the $V_z \times B_\theta$ force and since the plasma does not completely neutralize the beam current, the net result is the pinching of the beam. As stated by Joshi *et al.* (1987), the angular spread of a beam can be estimated quantitatively from the betatron motion of individual particles so that, if the betatron wavelength is approximately equal to $\beta \simeq 2\pi[\gamma mc^2 r/(-F_r)]^{1/2}$, the beam angular spread of $(\Delta\theta)_\beta = 2\pi r/\beta$ results from the betatron oscillations. For the ILSF storage ring beam parameters in Table 1, the angular spread of the beam in the presence of a plasma with $n_0 = 6.2 \times 10^{16} \text{cm}^{-3}$ is $(\Delta\theta)_\beta = 6.28 \times 10^{-6} \text{rad}$. This value is too small to affect the beam emittance.

In the new generation of light sources and FELs, the electron beam emittance and the energy spread are smaller than 400 pm and 0.2%, respectively. Degradation of the electron beam quality increases the energy spread and the emittance and decreases the photon beam brilliance. In conclusion, the plasma density should be chosen so that, despite the detrimental effects of the beam–plasma interactions on the beam quality, the values of the beam emittance and energy spread remain within their acceptable ranges.

In addition to the instabilities and wake forces, the period length of an undulator can also affect the beam emittance and energy spread (Clarke, 2004). In MUs and MPUs, the period length is inversely proportional to the microwave frequency. In Fig. 3, the energy spread is plotted as a function of the microwave frequency for different plasma densities while considering the effects of Two-Stream and Weible instabilities, longitudinal wake force and undulator period length. The deflection parameter and the length of the undulator are $k = 2.06$ and $L = 100\lambda_u$, respectively, and the natural energy spread is equal to the natural energy spread of the ILSF storage ring beam, *i.e.* 6.79×10^{-4} . In Fig. 4, the emittance versus microwave frequency is plotted for different plasma densities while

Table 1
Electron beam characteristics of the ILSF storage ring.

Parameter	Value
Energy	3 GeV
Current	100 mA
Horizontal emittance	0.267 nm rad
Vertical emittance	0.00267 nm rad
Horizontal beam size	68.9 μm
Vertical beam size	2.96 μm
Vertical BSC	2.1 mm
Horizontal BSC	6 mm

considering the effects of Two-Stream and Weible instability, transverse wake force and undulator period length. From these two figures, it can be seen that, as the microwave frequency increases, the energy spread and the emittance increase. As mentioned before, increasing the microwave frequency decreases the period length, which in turn reduces the deflection parameter. To keep $k = 2.06$, it is essential to increase the microwave intensity. As the microwave intensity increases, the strength of the electromagnetic fields increases too. In spite of the fact that a stronger electromagnetic field can compensate the effect of period length reduction on the deflection parameter, it may degrade the beam quality.

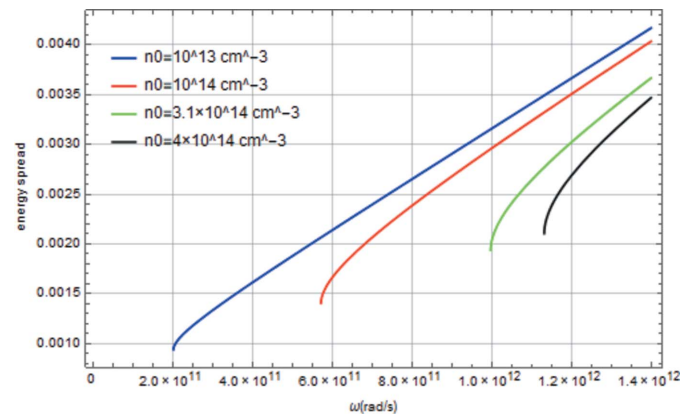


Figure 3
Energy spread variation versus microwave frequency for different plasma density.

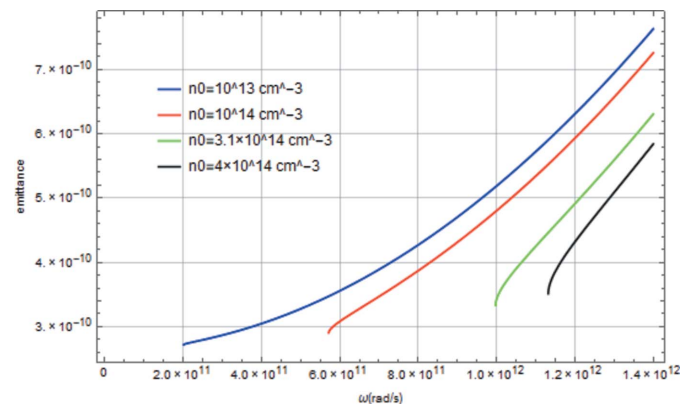


Figure 4
Emittance variation versus microwave frequency for different plasma density.

Table 2

Main parameters of the simulated MPU.

Parameter	Value
Waveguide dimensions	$a_0 = 6 \text{ mm}$, $b_0 = 2.1 \text{ mm}$, $l = 100\lambda_u$
Plasma density	$3.1 \times 10^{14} \text{ cm}^{-3}$
Operating frequency	160 GHz
λ_0	1.87 mm
λ_g	15.2 mm
λ_u	1.66 mm
Peak E_x on-axis	7.06×10^9
B_u	13.25
K_u	2.06

Considering Figs. 3 and 4, in order to keep the energy spread smaller than 0.002 and the emittance smaller than 0.4 nm rad, the maximum value of the microwave frequency for $n_0 = 3.1 \times 10^{14} \text{ cm}^{-3}$ is $10^{12} \text{ rad s}^{-1}$.

Another parameter to be considered in the study of beam dynamics in a storage ring is the damping time, τ . The fraction of the damping times with and without an MPU in a storage ring, *i.e.* τ_{MPU}/τ , for the MPU with the parameters in Table 2, is equal to 0.93, which indicates the minor effect of the MPU on the damping time.

In the following, the elliptical MPU with parameters listed in Table 2 is investigated, and its period length, synchrotron radiation flux and brilliance are calculated. Besides considerations about the beam quality degradation, the microwave frequency and the plasma density are chosen so that only the dominant mode of the waveguide is excited.

In Fig. 5, the electric field pattern of the microwave radiation along the elliptical plasma-filled waveguide axis is shown, in which the only present electrical field is along the y -axis. Therefore, the main oscillation of the electron beam is in the y - z plane, and the synchrotron radiation from this undulator has linear polarization.

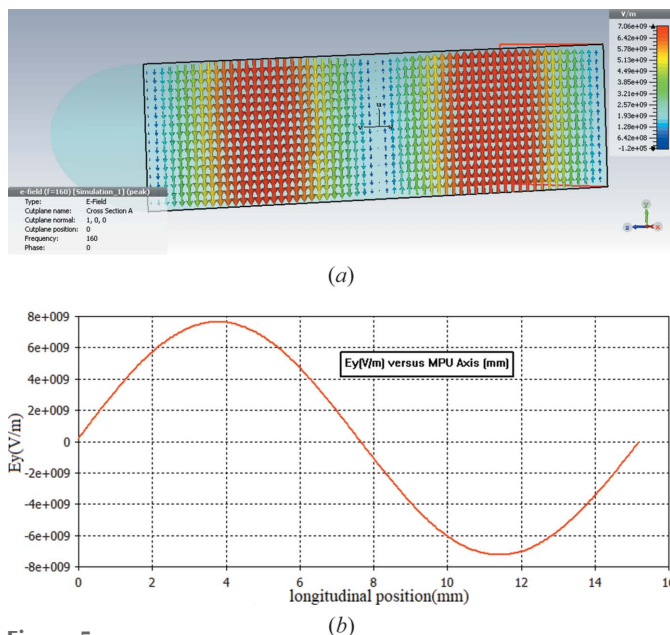


Figure 5 (a) Electric field pattern and (b) variation curve of the microwave radiation along the axis of the elliptical plasma-filled waveguide.

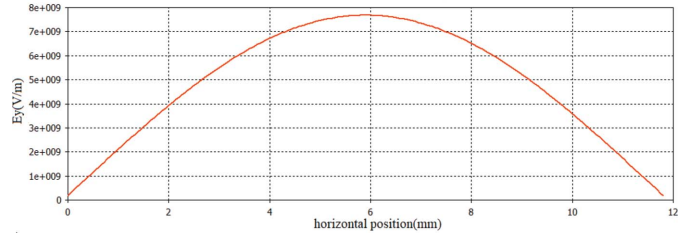


Figure 6 Electric peak field variation along the horizontal axis of the waveguide.

One of the main parameters to consider in designing insertion devices is the field roll-off in their good field region. The smaller the field roll-off, the smaller the values of the higher-order integrated multipoles will be. The higher-order integrated multipoles negatively affect the quality of the beam. In the ILSF storage ring, the horizontal good field region (GFR x) at the straight section (where the IDs are installed and dispersion is zero) is $\pm 0.7 \text{ mm}$. In Fig. 6, the horizontal roll-off is plotted. Field variations over the maximum field ($\Delta E/E_0$) over the $\pm 0.7 \text{ mm}$ is 2.42% which is an acceptable value for the field roll-off at the GFR.

Other essential parameters in designing IDs are the first and the second field integrals. Ideally, these integrals should be zero, which means the field's net effect on the beam is null. Nevertheless, in practice, these integrals are not zero. One of the main approaches to correct for the non-zero field integrals of an ID is to use corrector magnets at the end of it. These magnets could be used with MPUs as well.

It is worth mentioning that in conventional undulators, in which permanent magnets are used to create the required magnetic field, various factors such as the imperfections of the permanent magnets' block size and their magnetism as well as undulators construction imperfections result in deficiencies in the generated magnetic field. This can negatively affect the quality of generated synchrotron radiation and might result in brilliance reduction. The RMS phase error (σ_φ) is used by the IDs experts to investigate the effect of magnetic field deficiencies on the brilliance reduction. The brilliance reduction on the axis of IDs is shown by $R = \exp(-n^2\sigma_\varphi^2)$ in which n represents the radiation harmonic number (Walker, 2013). This reduction due to the RMS phase error is more drastic for higher harmonics that make it practically impossible to use harmonics higher than the seventh harmonic for a phase error larger than 5° (Clarke, 2004). Therefore, in light sources in which a wide synchrotron radiation energy range (*e.g.* 1 keV up to 40 keV) is covered with high harmonics, it is necessary to reduce the phase error as much as possible.

In Fig. 7, the flux and the brilliance of the elliptical plasma-filled waveguide are plotted. It can be seen that the first to seventh harmonics are covering the energy spectra ranging from 17 to 150 keV with flux higher than 10^{14} , and the energy spectra range from 17 to 180 keV with brilliance higher than 10^{20} . Comparing the results of Fig. 7 with the results of conventional undulators used to generate hard X-rays shows that the energy spectrum of the generated synchrotron radiation has increased significantly, and the flux and the

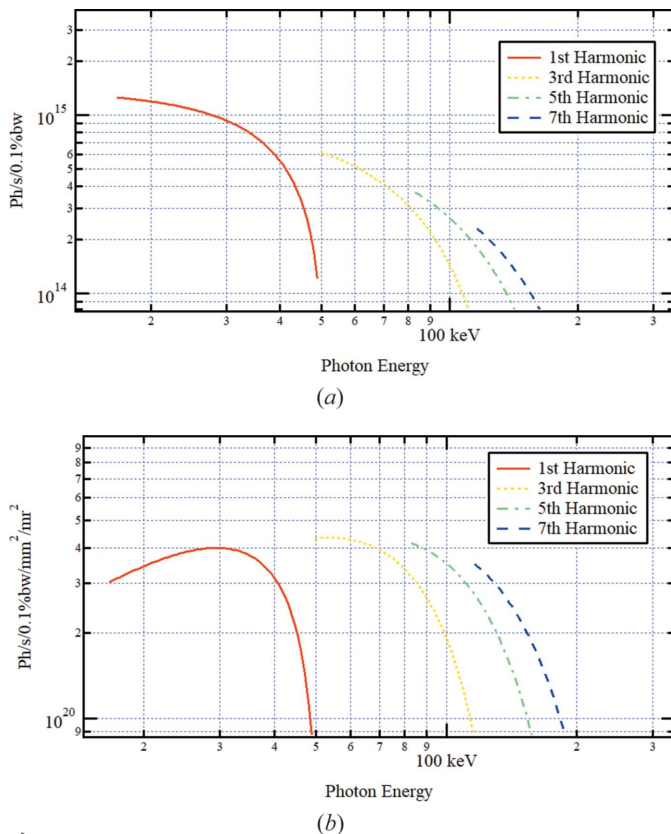


Figure 7
Tuning curve (a) and brilliance (b) of the elliptical MPU with the parameters in Table 2.

brilliance are increased by at least one order of magnitude. The ability of MPUs to generate synchrotron radiation with higher photon flux and brilliance is an evident and significant advantage over conventional undulators. This ability provides researchers with a chance to conduct more diverse experiments.

5. Summary and conclusion

In this paper, microwave propagation in a plasma-filled elliptical waveguide was studied. It was shown that this structure could work as a standard short-period undulator, *i.e.* an elliptical microwave plasma undulator (MPU). The propagation of TE modes in the waveguide was investigated, and the even and odd field components, cut-off frequencies and electron beam trajectory under the influence of electromagnetic fields of microwave radiation were calculated. With consideration of the electron beam dynamics and achieving a standard short-period elliptical MPU, the microwave frequency, the plasma density, and the undulator period length and deflection parameter were chosen. It was shown that the elliptical MPU eliminates the limitation of standard MUs in generating hard X-ray synchrotron radiation with overlapping harmonics, and it can generate higher photon flux with a wider energy spectrum compared with conventional MUs. The effects of beam–plasma interactions on the electron beam dynamics were studied, and the variations of the electron

beam emittance and energy spread versus microwave frequency for different plasma densities were plotted. The parameters of the electron beam inside the ILSF storage ring were used for radiation calculations.

It was also shown that MPUs have two significant advantages over conventional MUs, making their use in the storage ring of the new generation of light sources more efficient and more attractive. The first advantage of utilizing plasma, as an ionized medium, is that it does not undergo electrical breakdown and as a result it allows to increase the intensity of microwave radiation. In contrast, in vacuum waveguides, increasing the radiation power leads to electrical breakdown and system malfunctions. The possibility of increasing the radiation power gives the ability to maximize the magnetic field strength to maintain standard values for the deflection parameter, *i.e.* $K > 2$. Besides, the cut-off frequencies of the propagating modes of the microwave radiation in a plasma-filled waveguide are larger than the cut-off frequencies of the vacuum waveguides. So, as a result, it is possible to use microwaves with higher frequencies to reduce an undulators' period length without the necessity of exciting higher-order modes. Exciting higher modes negatively affects the electron beam dynamics and degrades the electron beam quality.

References

- Batchelor, K. (1986). *Proceedings of the 1986 International Linac Conference*, 2–6 June 1986, Stanford, CA, USA, p. 272.
- Bellucci, S., Bini, S., Biryukov, V., Chesnokov, Y., Dabagov, S., Giannini, G., Guidi, V., Ivanov, Y. M., Kotov, V. I., Maisheev, V. A., Malagù, C., Martinelli, G., Petrunin, A. A., Skorobogatov, V. V., Stefancich, M. & Vincenzi, D. (2003). *Phys. Rev. Lett.* **90**, 034801.
- Benabderrahmane, C., Valléau, M., Ghaith, A. P., Berteaud, L. C.-L., Chubar, O., Kitegi, C. & Couprie, M.-E. (2017). *Phys. Rev. ST Accel. Beams*, **20**, 033201.
- Chavanne, J., Hahn, M., Kersevan, R., Kitegi, C., Penel, C. & Revol, F. (2008). *Proceedings of the 11th European Particle Accelerator Conference (EPAC2008)*, 23–27 June 2008, Genoa, Italy, p. 2243.
- Chavanne, J., Penel, C., Plan, B. & Revol, F. (2003). *Proceedings of the 2003 Particle Accelerator Conference (PAC2003)*, 12–16 May 2003, Portland, OR, USA, p. 253.
- Clarke, J. (2004). *The Science and Technology of Undulators and Wigglers*. New York: Oxford University Press.
- Corde, S. & Ta Phuoc, K. (2011). *Phys. Plasmas*, **18**, 033111.
- CST Microwave Studio (2008). *CST Studio Suite*, <http://www.cst.com>.
- Hara, T., Tanaka, T., Kitamura, H., Bizen, T., Maréchal, X., Seike, T. & Matsuura, Y. (2004). *Phys. Rev. ST Accel. Beams*, **7**, 050702.
- Huang, J., Wu, L., Yang, C., Chuan, C., Chung, T. & Hwang, C. (2014). *Appl. Supercond.* **24**, 0503704.
- Huang, J.-C., Kitamura, H., Yang, C.-K., Chang, C.-H., Chang, C.-H. & Hwang, C.-S. (2017). *Phys. Rev. Accel. Beams*, **20**, 064801.
- Joshi, C., Katsouleas, T., Dawson, J., Yan, Y. & Slater, J. (1987). *IEEE J. Quantum Electron.* **23**, 1571–1577.
- Kitamura, H. (1995). *Rev. Sci. Instrum.* **66**, 2007–2010.
- Krall, N. & Trivelpiece, A. (1973). *Principles of Plasma Physics*. New York: McGraw-Hill.
- Kuzikov, S., Jiang, Y., Marshall, T., Sotnikov, G. & Hirshfield, J. (2013). *Phys. Rev. ST Accel. Beams*, **16**, 070701.
- McLachlan, N. (1951). *Theory and Application of Mathieu Functions*. London: Oxford University Press.
- Onuki, H. & Elleaume, P. (2003). *Undulators, Wigglers and their Applications*. London: Taylor & Francis.

- Pellegrini, C. (2005). *Proceedings of the 27th International Free Electron Laser Conference (FEL2005)*, 21–26 August 2005, Stanford, CA, USA, p. 203.
- Rykovanov, S., Schroeder, C., Esarey, E., Geddes, C. & Leemans, W. (2015). *Phys. Rev. Lett.* **114**, 145003.
- Smirnov, B. (2015). *Theory of Gas Discharge Plasma*. London: Springer Cham.
- Tanaka, T., Hara, T., Bizen, T., Seike, T., Tsuru, R., Maréchal, X., Hirano, H., Morita, M., Teshima, H., Nariki, S., Sakai, N., Hirabayashi, I., Murakami, M. & Kitamura, H. (2006). *New J. Phys.* **8**, 287.
- Tantawi, S., Shumail, M., Neilson, J., Bowden, G., Chang, C., Hemsing, E. & Dunning, M. (2014). *Phys. Rev. Lett.* **112**, 164802.
- Walker, R. (2013). *Phys. Rev. ST Accel. Beams*, **16**, 010704.
- Wong, C. S. & Mongkolkeha, R. (2016). *Elements of Plasma Technology*. Singapore: Springer.
- Zhang, L., He, W., Clarke, J., Ronald, K., Phelps, A. D. R. & Cross, A. (2019). *J. Synchrotron Rad.* **26**, 11–17.